VORTICAL FLOW MANAGEMENT FOR IMPROVED CONFIGURATION AERODYNAMICS - RECENT EXPERIENCES

Dhanvada M. Rao
Vigyan Research Associates, Inc.
28 Research Drive
Hampton, VA 23666, U.S.A.

SUMMARY

This paper reports recent progress in vortex-control applications for alleviating the adverse consequences of three-dimensional separation and vortical interactions on slender body/swept wing configurations. Examples include: helical separation trip to alleviate the side force due to forebody vortex asymmetry; hinged strakes to avoid vortex breakdown effects; compartmentation of swept leading-edge separation to delay the pitch-up instability; under-wing vortex trip and vortex flaps for drag reduction at high lift; and an apex-flap trimmer to fully utilize the lift capability of trailing-edge flaps for take off and landing of delta wings. Experimental results on generic wind-tunnel models are presented to illustrate the vortex-management concepts involved and to indicate their potential for enhancing the subsonic aerodynamics of supersonic-cruise type vehicles.

NOMENCLATURE

C_L	Lift coefficient	C_Y	Side force coefficient
C_l	Rolling moment coefficient	C_t	Local leading-edge thrust coefficient
C_{l_β}	Lateral stability derivative, $\partial C_l/\partial\beta$	L/D	Lift-to-drag ratio
C_m	Pitching moment coefficient	α	Angle of attack
C_n	Yawing moment coefficient	β	Angle of sideslip
C_{n_β}	Directional stability derivative, $\partial C_n/\partial\beta$	δ	Control deflection angle
C_p	Pressure coefficient	η	Spanwise coordinate normalized by semi-span

1. INTRODUCTION

The expanding flight and maneuvering envelopes demanded by recent tactical aircraft design studies have resulted in a growing awareness of the need to understand and to work with massive three-dimensional separations and the associated vortical flows. Slender bodies and highly-swept wings in combination generate a kaleidoscope of complex vortex systems through the angle of attack range, whose implications increasingly concern the configuration aerodynamicist. Equally, they offer an unique opportunity for utilizing the energy and persistence of these vortical structures in innovative ways to engineer the aerodynamic characteristics for improved flight capability and extended operational limits.

This paper is a progress report of continuing research at NASA Langley Research Center, aimed at conceptualizing practical means of vortex-flow manipulation to upgrade the subsonic performance, stability and control characteristics of the new generation supersonic-cruise tactical aircraft. Selected examples from recently published results of this work will be presented, to indicate the broad scope of the problem areas being addressed with the underlying theme of re-structuring a problematical separated flow condition through artificially-generated vortex systems, as opposed to the conventional approach of suppressing flow separation. Only the basic concepts and their experimental evaluation can be discussed within the present space limitations; additional results indicating the scope of applications of the concepts can be found in the referenced literature. This paper complements a preceding NASA Langley paper (ref. 1).

2. HELICAL TRIPS

The onset of asymmetry in the forebody vortices at high angles of attack produces an abrupt side force (and yawing moment) which can be highly adverse to the aircraft handling characteristics at maneuvering limits. This asymmetry is believed to arise from an unstable interaction between the counter-rotating primary vortices when they are in close proximity to each other, but away from a solid boundary. While research continues for a better understanding of the basic fluid mechanism involved and to predict the onset and magnitude of side force, it is of interest to devise practical means to eliminate or control the phenomenon which can be a limiting factor in high-alpha maneuvering of aircraft and missiles. A passive, add-on device is preferred which will alleviate the side force on any given forebody shape without inducing undesirable side effects on performance or stability. The well known nose strakes generate vortex systems of their own which, in a manner not yet fully understood, force the forebody wake to remain symmetrical to higher angles of attack. However, experience with nose strakes shows that their effectiveness is highly dependent on the forebody shape and therefore a trial-and-error development of the optimum strake is required for every new application; they also frequently produce adverse changes in the lateral-directional characteristics at high angles of attack. Nose-radome mounted strakes in addition are likely to interfere with radar performance. Nevertheless, the low drag penalty and ease of installation are positive advanteges that motivate the search for more universally applicable forms of nose strakes, which are also free of the adverse side effects mentioned above.

The helical-trip device (fig. 1) represents an approach that is conceptually different from the conventional strakes: it seeks to prevent the formation of a coherent vortex pair from forebody separation and thus to eliminate the possibility of asymmetry altogether. The means adopted for this purpose was suggested by the mechanism of suppression of the alternate vortex shedding from cylinders in cross-flow, ref. 2 . The helical trips were accordingly devised to force separation at varying peripheral locations along the forebody length to generate a non-uniform feeding sheet and thereby impede the roll-up into concentrated vortex cores, while maintaining a "mirror-image" symmetry of trips with respect to the pitch plane to avoid any direct trip-induced side force. The selected helix orientation placed the trip nearly transverse to the boundary-layer flow at high angles of attack, thus making it more effective in provoking separation.

The concept was evaluated on a series of wind-tunnel force models ranging from basic axi-symmetric bodies (cone- and ogive-cylinders), through fuselage shapes with vertical and horizontal oval cross-section, to wing/fuselage/tail combinations representing a generic fighter configuration (ref. 3). The results shown in fig. 2 are supportive of the helical trip concept:

i) straight side-trips (B) do not appreciably change the basic fuselage side force characteristics (A);
ii) helical trips (C), made from the same wire material as (B), suppress the side force up to the highest alpha;
iii) inverted helical trips (D), obtained by rolling the forebody through 180°, totally lose their capability (since they are now approximately parallel to the boundary layer flow);
iv) truncated helical trips (E), possibly to further reduce radar interference, basically remain effective; and
v) 50-percent reduction in helical trip diameter (F) does not degrade the trip capability until approaching the highest alpha.

Since the trip height will be scaled with the boundary-layer thickness, in full-scale applications the relative trip size will be much smaller than the size tested on the wind tunnel models. It is noteworthy that on all the test bodies, the very first helical trip application was effective, no subsequent adjustment being required of the initial trajectory shape used. This lack of sensitivity to the trajectory shape is consistent with the helical-trip hypothesis, apart from being an advantage in practical applications.

Helical trips were further evaluated during a NASA Langley study of forebody shape effects on the lateral/directional as well as longitudinal stability at high angles of attack of a contemporary fighter configuration with extended forebody (ref. 4). The helical-trip effectiveness results presented in fig. 3 show that the high-alpha yawing moments were alleviated generally without degrading the lateral-directional stability characteristics. A further consideration (ref. 4) was the yaw-induced pitching moment during high-alpha maneuver when the pitch-down authority of the longitudinal controls may become marginal. A direct comparison of conventional nose-strakes and helical trips (fig. 4) shows that whereas the addition of strakes results in an adverse nose-up moment in sideslip, helical trips actually produce a favorable trend relative to the "clean" forebody. These results serve to emphasize the basic difference between the two devices: the helical trips achieve side-force suppression by disrupting the forebody vortices thus avoiding the undesirable vortex-triggered side effects, as opposed to vortex intensification by the conventional nose strakes.

3. HINGED STRAKES

Wing strakes are highly-swept root extensions of the leading-edge whose function is to generate strong vortices at high angles of attack in order to re-energize the stalling flow over the wing and thereby improve the maximum-lift capability. The strake vortices generally have sufficient lateral separation to preclude the unstable mutual interaction associated with forebody vortices; however, they individually are subject to the well-known breakdown phenomenon. When vortex breakdown occurs over the wing, an abrupt loss of its beneficial influence leads to stall, pitch-up and roll/yaw disturbances. Being a dynamic phenomenon, vortex breakdown also instigates buffet and associated undesirable motions such as wing rock, noseslice etc. The expansion of wing wake following strake vortex breakdown degrades the effectiveness of aft-tail surfaces, and may result in serious loss of controllability. Automatic limitation of the angle of attack envelope in order to stay below the vortex-breakdown boundary restricts the maneuver potential of the vehicle and is not a preferred solution. The hinged-strake concept was devised as a means to suppress the strake vortices and thus to eliminate the vortex-breakdown boundary altogether; in addition, articulated strakes offered the possibility of improving post-stall maneuverability when the control power of conventional surfaces has degraded.

The hinged strakes, structurally separate from the wing, are attached to the fuselage through longitudinal hinges (fig. 5). In the normal co-planar position the strakes function conventionally. At high angles of attack approaching vortex breakdown, however, they may be rotated downwards to an anhedral angle. Increasing anhedral not only decreases the strake projected planform area but also the normal force coefficient by reducing both the linear and the non-linear contributions (ref. 5), thus providing an effective control over the strake loading as well as on its vortex characteristics. Examples of strake anhedral effects on the high-alpha aerodynamics of a generic fighter configuration (fig. 6) will be presented through some results of a low-subsonic wind tunnel study (ref. 7). In order to highlight the anhedral effects, relatively large strakes (of exposed area = 26.6% of wing reference area) were selected for this investigation.

The lift and pitching-moment characteristics of the wing/fuselage/vertical fin configuration (without a horizontal tail) having strakes at 30 deg. anhedral are shown in fig. 7, in comparison with planar strake data (ref. 6). The onset of vortex breakdown with the planar strake is evidenced by a peaking of C_L accompanied by pitch-up and lateral/directional disturbances as the angle of attack approaches 30 degrees. These vortex breakdown effects can be seen to be greatly alleviated with the anhedral strakes. Suppression of vortices coupled with the reduced projected area of anhedral strakes inevitably penalizes the maximum lift relative to planar strakes of equal surface area. However, when compared with data for planar strakes of smaller i.e. 16.5% area (ref. 6) where pitch-up limits the usable C_L to 1.2 approx. (at α = 19 deg.),

the anhedral strakes are seen as an improvement with a maximum C_L of 1.5 (at α = 42 deg.) free of pitch-up. Thus, hinged-strakes of suitably increased size in an anhedral setting can allow high-alpha maneuvering free of vnrtex breakdown problems and without sacrificing the maximum lift capability of the conventional fixed strakes.

The planar-strake vortex effects also cause non-linearity in the rescoring moment characteristics of the horizontal tail, as indicated in fig. 8. In the low-alpha range, addition of planar strakes to the strake-off configuration reduces the horizontal-tail effectiveness due to increased downwash behind the wing. Vortex breakdown and associated reduction in the downwash then leads to a rapid increase in $\Delta C_{m,HT}$ slope around α = 30 degrees. An absence of this non-linearity in the hinged-strake data, which closely duplicates the strake-off characteristics, is further evidence of vortex suppression due to strake anhedral. As a result, up to 50% increase in horizontal-tail effectiveness is obtained in the mid-alpha range by employing anhedral rather than planar strakes.

Effective pitch-down capability is important for a positive and rapid recovery from extreme nose-high attitudes during post-stall maneuvering, an area where aft-tail pitch controls are usually found lacking due to wake effects. On the other hand, the strake loading not only continues to increase to high angles of attack but also acts well forward of the aircraft c.g. Consequently, the use of hinged strakes for pitch recovery appears worth considering. The incremental nose-down moment due to symmetrically articulated strakes at 30 deg. and 45 deg. anhedral is shown in fig. 9, together with strake-off data which may be supposed to represent the limiting case of 90 deg. anhedral. Also shown for comparison is the result taken from ref. 8 for an aft-tail fighter configuration with maximum nose-down stabilator deflection, which displays the typical loss of effectiveness starting at α = 25 deg. Evidently the hinged strakes can provide a powerful and fully controlled nose-down moment for recovery from very high angles of attack.

Considering now the asymmetric articulation mode, e.g. only the right-hand strake deflected, a positive rolling moment is obtained due to the larger lift on the left-wing panel which is still under the influence of the planar-strake vortex. As shown in fig. 10, the rolling moment coefficient increases quadratically with angle of attack for a given strake deflection until the onset of the planar-strake vortex breakdown, i.e. α = 28°. Up to this angle of attack, the induced yawing moment (resulting from the forebody side-force generated by the right-strake deflection) is favorable. After vortex breakdown the rolling moment rapidly decreases and the yawing moment becomes adverse; however a substantial roll power is still available at high angles of attack in comparison with the conventional ailerons. Also shown in fig. 10 are the results for another vortex-related roll control concept viz. spanwise blowing on one wing panel (ref. 9). Although the rolling moment characteristics in this case are very similar to the asymmetrically deflected hinged strake, the induced yaw unfortunately is adverse and equal in magnitude to the rolling moment throughout the alpha range.

4. 'COMPARTMENTATION' OF SWEPT LEADING-EDGE SEPARATION

The predilection for early separation off highly-swept leading edges offers a rewarding field for the application of vortex flow control concepts. From the onset of leading-edge separation, a rapid collapse of leading-edge suction with increasing angle of attack aggravates the lift-dependent drag; with the progressive inboard movement of leading-edge vortices the tip sections lose the benefit of vortex lift resulting in pitch instability, which is of special concern in relaxed static stability applications to tail-less configurations.

This section deals with a leading-edge 'compartmentation' concept which aims to restrain the inboard spread of separation by means of fixed leading-edge devices. The swept leading edge is divided into aerodynamically isolated compartments, each having attached flow at its inboard end while the growth of leading-edge separation is confined to the compartment span. Consequently, at a given angle of attack the scale of separation averaged over the span is reduced in comparison with the original wing. At the same time, the vortex migration out of the tip region is retarded thus improving the tip lift characteristics. The postulated compartmentation of the leading-edge separation is sketched in fig. 11.

The compartmentation concept was evaluated in low-subsonic tests on 60-deg. and 74-deg. delta wing models. The leading-edge devices used for the purpose were fences, chordwise slots and pylon-type vortex generators. The pressure-instrumented leading edge on the 60 deg. delta model allowed the compartmentation effect to be monitored via the spanwise distribution of leading-edge pressure coefficient ($C_{P,L.E.}$), as illustrated in fig. 12. With the basic wing leading edge substantially separated at α = 18.7 deg., the fence as well as the slot reduce the separation outboard of their location as indicated by the raised leading-edge suction levels, the fence showing a stronger effect than the slot at this high angle of attack. Further compartmentation of the leading edge by means of three equally-spaced slots is shown in fig. 13. The increased average leading-edge suction level due to multiple compartmentation results in drag reduction above α = 11 degrees (when the basic wing has become significantly separated), which is reflected in the L/D comparison of fig. 14A. At a given C_L however the L/D is hardly improved (fig. 14B), because suppression of leading-edge separation also reduces the vortex lift, which must be compensated by increasing the angle of attack resulting in a drag increment. This is an intrinsic limitation on the use of leading-edge separation control (regardless of the means employed) for L/D improvement on wings where leading-edge vortices contribute significantly to lift.

The second purpose of compartmentation, i.e. to retard the inboard migration of the leading-edge vortex, is illustrated for the same three-slot configuration in fig. 15, which plots the upper-surface pressure coefficient at a representative tip location versus angle of attack. The compartmentation effect increases the angle of attack corresponding to the vortex passage over the reference point (as identified by the -CP peak) from 12.5 deg. on the basic wing to 19.5 deg. with the slots. The later departure of the vortex from the tips is directly reflected in a delayed pitch-up observed in pitching-moment characteristics, fig. 15. Additional information and data on the performance of other slot and fence arrangements on the 60-deg. delta model will be found in refs. 10-12.

The pylon-type vortex generator (PVG) resembles a scaled-down pylon projecting down and forward from the leading edge (fig. 16). This arrangement was intended to exploit the prevailing sidewash near the swept leading edge for generating a streamwise vortex off the top edge of the pylon, the vortex rotation being such as to induce a downwash on the outboard side. The increasing sidewash with angle of attack intensifies the vortex, resulting in augmentation of downwash which will tend to keep the leading edge attached adjacent to and outboard of the PVG location (fig. 17). Thus the compartmentation effect should be maintained to high angles of attack when the previous devices (fence and slot) begin to fail.

The persistence of the compartmentation due to pylon vortex generators may be judged by the 60 deg. delta spanwise leading-edge pressure distribution at 22.5 deg. angle of attack (the maximum of the test) with three equi-spaced devices, fig. 18, in comparison with a three-slot arrangement. The corresponding pitching-moment characteristics, fig. 19, show a strong stabilizing influence due to the vortex generators. A further demonstration of the pylon effectiveness in improving the longitudinal stability of 74 deg. delta wing is shown in fig. 20, this time in comparison with fences (ref. 13). It should be stressed that the PVG arrangements employed in these tests were by no means optimum, and that more efficient spanwise locations might be found for specific planforms.

5. UNDERWING VORTEX TRIP

While compartmented-separation is found to be an effective means of improving the longitudinal stability of highly-swept configurations, its potential for drag reduction at high angles of attack may be limited on thin, small-radius leading edges typical of supersonic cruise wings. At the same time, the cruise drag penalty of multiple fixed devices may be unacceptable. Alternatively, for retractable systems light weight and short travel are important considerations to allow rapid actuation during high-speed tactical maneuvers. These requirements, as well as the need for effective leading-edge thrust capability on thin wings to high angles of attack, appear to be met by the underwing vortex trip, fig. 21. This flap-like device opens to create a forward-facing cavity under the leading edge. Forced separation at the sharp forward edge of the flap feeds a spanwise spiralling vortex situated at the mouth of the cavity. The vortex suction acting over the cavity frontal area produces thrust all across the cavity span. An optimally placed vortex will induce the outer flow to turn parallel to the upper surface thus remaining attached on the wing, regardless of the leading-edge radius. The adjustable flap will allow control of the vortex position as a function of angle of attack, in order to maximize the thrust effectiveness over the alpha range.

For simplicity during a preliminary investigation of the concept, the underwing vortex trip was simulated by means of a thin, swept flat plate secured to the bottom surface of the 60-deg delta model (ref. 10-12). This plate projected parallel to the wing plane and terminated directly below the leading edge, leaving a gap between the plate and the wing lower surface (see sketch in fig. 22). While this fixed geometry restricted the scope of the investigation to a single (and not necessarily optimum) trip position, the results still are of interest as they reveal the mechanism underlying the drag-reduction capability of the concept.

A set of chordwise pressure distributions around the leading edge at the highest angle of attack of the test (i.e. α = 22.5 deg.) presented in fig. 22 show the vortex-trip induced suction replacing the positive pressure region on the lower surface of the basic wing leading edge (shaded area). The spanwise distribution of the local thrust coefficient obtained by integrating these pressure distributions show that the thrust with the vortex trip is more than twice that on the basic leading edge, fig. 23. The effect on L/D is shown in fig. 24, which also indicates the theoretical boundaries for the delta wing assuming 100-percent leading edge thrust (fully-attached flow) and 0-percent thrust (fully-separated vortex flow). In comparison with the lower boundary, it is seen that the basic wing retains a fair degree of residual thrust even after separation due to the relatively blunt leading edges (see fig. 23); consequently the L/D-increment due to the vortex trip appears rather small. However, since the leading-edge radius is irrelevant to its aerodynamic mechanism, the vortex trip should function equally well under a sharp leading edge given an equivalent frontal area of the cavity. Therefore, the L/D-increment relative to the zero-thrust boundary should be a fairer assessment of the vortex-trip capability. While the present results serve to verify the basic hypothesis of the concept, further studies on a thin wing whith variable trip deflection will provide a better indication of the drag-reduction potential of vortex trips at high lift coefficients.

6. VORTEX FLAPS

Unlike the conventional leading-edge flaps for maintaining attached flow at high angles of attack, the vortex flap is designed to operate with separation on its upper surface. When employed on a highly swept wing the three-dimensional separation is stabilized by a spanwise-spiralling vortex, whose concentrated suction acting on the forward-sloping flap surface generates a thrust component (fig. 25). While it may also serve in the conventional sense at the lower angles of attack (or on less-swept leading edges) where attached flow is feasible, the unique ability of the vortex flap to function effectively under an organized and stable separated flow renders it less sensitive to off-design conditions. This feature is particularly advantageous on slender wings which operate through a large angle-of-attack range and have a pronounced spanwise variation in the leading-edge upwash. In addition, the vortex-induced re-attachment at or near the hinge line helps to suppress hinge-line separation which can be a limitation with the conventional leading-edge flaps.

Since the first experimental demonstration of the drag-reduction potential of the vortex flap concept (ref. 14), a sizeable data base has been generated (refs. 15-26). In this section, some recent results from on-going research at Langley will be presented to support a discussion of area-efficient vortex flaps.

Originally conceived for use on supersonic transports to allow approach and landing with reduced engine thrust (for airfield noise alleviation), the vortex flap was to be deployed (Kreuger fashion) from

a nested position on the wing under-surface, i.e. in an area-extending mode, (fig. 25). Currently, there is considerable interest in combat aircraft applications of the vortex flap to improve the sustained-g performance in high-speed maneuver. For such applications a rapid-deflection capability as with the conventional leading-edge flaps would obviously be more desirable. However, the integration of vortex flaps with their relatively large chord is structurally difficult within a slender wing planform and also leads to an aerodynamic performance penalty. As an illustration of the aerodynamic problem, two sets of L/D results with vortex flaps of nearly equal area and at 30 deg. deflection on a 74 deg. delta wing are compared in fig. 26: one pertaining to "extending" flaps where the basic wing reference area (i.e. excluding flaps) is used (ref. 14), and the other for "integral" flaps where the reference area includes the flaps (unpublished Langley data). Although in both cases the vortex flaps generated nearly the same aerodynamic thrust (as confirmed by their axial force characteristics, not shown), the L/D increments are far less in the "integral" case. This is because for a given lift coefficient, say C_L = D.5, a higher angle of attack is needed with integral flaps (viz. 16.5 deg. versus 14.6 deg. for extending flaps), and the consequent drag increase significantly penalizes the L/D improvement. Although trading vortex lift for thrust is central to the vortex flap concept, with integral flaps not only the vortex lift but also some linear lift is lost on slender wings (ref. 5), whereas the additional area provided by extending flaps is able to largely compensate for the loss of linear lift.

The above example serves to emphasize the importance of reducing the integral vortex flap area without unduly sacrificing its thrust, for obtaining useful L/D improvements. The possibilities in this regard are suggested by the spanwise variation in flap thrust contribution as determined by the vortex development. A typical case is illustrated in fig. 27, where the upper-surface pressure distributions at five spanwise stations on the 74 deg. delta wing are used to infer the local aerodynamic loading and the associated flow patterns. Flap deflection is seen to lower the suction level inboard of the hinge line well below the planar wing levels throughout the span, which coupled with the smaller effective wing area is responsible for a marked lift reduction. The varying average suction level on the flap upper surface indicates a wide-ranging thrust effectiveness at the different stations. In particular, at station (A) a largely attached flow is obtained inboard of a localized leading-edge vortex (which lies just outside the first pressure tap), thus the flap chord here contributes negligible thrust. The flap utilization is improved considerably, however, at stations (B) and (C) where the vortex has expanded to nearly match the flap chord. Thereafter, continued vortex enlargement progressively drives the peak suction and the re-attachment inboard across the hinge line, stations (D) and (F) indicating successive reductions of the flap thrust as well as increasing drag due to spreading of the vortex suction foot-print onto the wing. A planview projection of the suction peak and re-attachment positions inferred from the upper-surface pressure distributions in fig. 27 graphically presents the vortex track and its expansion down the wing. A large, obviously unproductive region of this flap (shaded area) may be eliminated by means of a gothic-shaped apex. Further, by a suitable re-structuring of the vortex to delay its inboard migration, the thrust contribution of the outer regions of the flap may be improved.

A preliminary trial of the above qualitative ideas was included in a recent Langley test program, (ref. 24), using a 58 deg. delta wing/fuselage model originally fitted with a constant-chord vortex flap (fig. 28, A), which also shows the successive modifications of the original flap. The corresponding L/D characteristics, fig. 28, B attest to the improvements accompanying the flap modifications (at a constant deflection of 40 deg.). A relatively small alteration of the apex from its original low-sweep to the gothic shape improves the vortex initiation and renders the apex region more thrust effective, leading to a striking increase in L/D up to C_L = 0.6. Introduction of a snag was intended to arrest the flap vortex at a part-span discontinuity and, with the help of a counter-rotating snag vortex, to retard its inboard migration. At the same time, the flap chord inboard of the snag was substantially reduced to match the much smaller vortex in this region. These modifications to the flap shape further improved the L/D up to C_L = D.6. An alternative approach (to the snag) considered for maintaining the thrust effectiveness of outboard flap region was to strengthen the vortex feeding sheet at a part-span position by a local sweep reduction, which was simply obtained by removing the snag. The results show that the L/D improvement at higher lift coefficients was retained with the final shape, while achieving a 25% flap area reduction relative to the original constant-chord flap. The pitching-moment characteristics (fig. 28, C) associated with these flap modifications for L/D improvement show simultaneous benefits in the longitudinal stability, which is an equally important consideration in maneuvering applications.

At this writing, an aggressive program to explore further refinements of the basic vortex flap concept (refs. 25, 26) and to develop design tools is in progress at NASA Langlay and within the industry, and it is likely that the next generation tactical aircraft designs will utilize advanced forms of leading edge vortex manipulation concepts.

7. APEX FLAP

The restriction on angle of attack to ensure adequate forward view as well as to avoid tail scraping on slender wing aircraft, denies access to the non-linear lift and consequantly limits the lift capability during take off and landing. The lift contribution of trailing-edge flaps on such aircraft also is generally limited by the available trim power, particularly on tail-less configurations. Augmentation of the trim capability by using canard surfaces must accept a supersonic drag penalty; on the other hand, retractable canard devices are mechanically complex and cannot usually be deployed during high speed maneuvering.

Lift enhancement on highly swept wings at low angles of attack by means of forced vortices has been considered, two such concepts being the inverted vortex flap (ref. 23) and the upper vortex flap (ref. 25), fig. 29. Wind tunnel tests with these devices indicate a lift-increment potential of ΔC_L = 0.06 on a 74-deg. delta wing; even this modest lift increase requires quite large vortex-generating flaps, approaching 25% of the wing area. Apart from practical considerations, these large flaps produce drag levels that may be excessive during take off.

This section discussas an apex flap concept for delta wings which also relies on forced vortices, fig. 29. The apex flap however is intended primarily as a controllable lifting trimmer (like a canard) to permit the full utilization of trailing-edge flap potential at low angles of attack. The undeflected

apex flap becomes an undistinguishable part of the high-speed wing configuration and therefore incurs no cruise-drag penalty. Since the apex flap generates a large amount of vortex lift well forward of the center of gravity, a relatively small flap area (viz. 10% or less of the wing) can provide a powerful trim effect, in addition to its own direct lift. The possibility of obtaining some additional lift from the induced suction of the apex vortices passing over the main wing surface lends further interest to apex flap concept.

A basic study was performed on a 74 deg. flat-plate delta wing, incorporating a transverse hinge line at 25% center chord to obtain a 6% area apex flap and also trailing-edge flaps of comparable area (ref. 27). Flow visualizations revealed three basic vortex-patterns as sketched in fig. 30 in the order of increasing angle of attack with constant apex flap deflection; most frequently encountered was the 'merged' vortex pattern, probably due to the high leading-edge sweep of the subject wing.

The apex-flap trim capability is indicated by comparing the opposing pitching-moment increments generated by the apex and the trailing-edge flaps, fig. 31, according to which an almost-trimmed condition is achieved fortuitously with equal deflections of the two flaps up to α = 20 degrees. The trimmed-lift curve generated by the 20 deg/20 deg. flap combination (fig. 32) allows a 4 deg. reduction in angle of attack (or a ΔC_L = 0.12) relative to the planar wing. As shown in fig. 32, this trimmed configuration incurs no L/D penalty at $C_L \geq 0.5$ in comparison with the planar wing.

Above 20 deg. deflection the trailing-edge flap ΔC_m curve (fig. 31) indicates a progressive loss of its effectiveness (due to extensive flow separtion on the flap as confirmed by oil flow), whereas the apex-flap moment increment continues unabated to nearly 30 deg. deflection. Thus, the trimmed-lift increment shown in fig. 32 is limited not by the apex flap but rather the trailing-edge flap. The excess trim capability of the apex flap might therefore be further exploited for instance, by controlling the trailing edge flap separation and thus extending its effectiveness to higher deflection angles. A potential flow calculation of the trailing-edge flap characteristics gives the upper-limit of improvement if attached flow were maintained up to δ = 30 deg., fig. 33. The corresponding C_L (trim) curve, using apex-flap experimental ΔC_m data, then indicates a substantial improvement at low alpha, fig. 34.

The apex flap lift coefficient based on apex area, deduced from the measured axial-force increment due to flap deflection, at various deflection angles is plotted versus the apex angle of attack relative to free stream ($\alpha + \delta$) in fig. 35. For comparison, lift data for a 74 deg. delta wing (ref. 28) is also given, which shows the vortex breakdown effect at α = 35 deg. Contrary to the expectation of an earlier vortex breakdown at the hinge line, the apex lift curves do not indicate any evidence of it even with the ($\alpha + \delta$) approaching 60 degrees. Smoke visualizations of the apex vortices in the hinge-line plane also did not show the typical characteristics associated with vortex breakdown up to the extreme apex flap deflection and angle of attack. A satisfactory explanation of this observation is lacking; however, the sustained aerodynamic effectiveness of the apex flap makes it a potentially powerful control surface for high alpha applications. As such, further investigation of the concept and its integration into fuselage-wing configurations appears worth pursuing.

8. CONCLUDING REMARKS

A number of vortex-control devices were conceptualized and investigated experimentally as possible solutions to a range of high-alpha aerodynamic problems of slender and highly-swept configurations. Specifically, forebody side force triggered by vortex asymmetry, post-stall maneuvering limitations due to strake vortex breakdown, pitch-up resulting from the migration of leading-edge vortices away from the tips, excessive lift-dependent drag due to loss of leading-edge suction and vortex lift, and lift limitation at take off and landing were addressed. In each case a practical approach was demonstrated for vortex manipulation to eliminate the problem or to reduce its severity. While the devices described in this paper are interesting in themselves, the experience of formulating certain hypotheses relating to vortex behaviour and putting them to test has proved valuable towards refining our insights into the relatively new field of vortex aerodynamics.

REFERENCES

1. Lamar, J. E. and Campbell, J. F.; "Recent Studies at NASA-Langley of Vortical Flows Interacting with Neighbouring Surfaces." 1983, AGARD Symposium on Aerodynamics of Vortical Type Flows in Three Dimensions, Paper No. 1D.

2. Naumann, A., Marsbach, M. and Kramer, C.; "The Conditions of Separation and Vortex Formation Past Cylinders," 1966, AGARD CP4, pp. 547-574.

3. Rao, D. M.; "Side Force Alleviation on Slender, Pointed Forebodies at High Angles of Attack." J. Aircraft, Vol 16, No. 11, Nov. 1979.

4. Carr, P. C. and Gilbert, W. P.; "Effects of Fuselage Forebody Geometry on Low-Speed Lateral-Directional Characteristics of Twin-Tail Fighter Model at High Angles of Attack." 1979, NASA TP 1592.

5. Kuchemann, D.; "The Aerodynamic Design of Aircraft." Pergamon Press, 1978.

6. Luckring, J. M.; "Subsonic Longitudinal and Lateral Aerodynamic Characteristics of a Systematic Series of Strake-Wing Configurations." 1979, NASA TM 78642.

7. Rao, D. M. and Huffman, J. K.; "Hinged Strakes for Enhanced Maneuverability at High Angles of Attack." J. Aircraft, Vol 19, No. 4, April 1982.

8. Nguyen, L. T., Gilbert, W. P. and Grafton, S. B.; "Control Considerations for CCV Fighters at High Angles of Attack." 1979, AGARD CP 262, Paper No. 11.

9. Erickson, G. E. and Campbell, J. F.; "Improvement of Maneuver Aerodynamics by Spanwise Blowing." 1977, NASA TP 1065.

10. Johnson T. D., Jr. and Rao, D. M.; "Experimental Study of Delta Wing Leading-Edge Devices for Drag Reduction at High Lift." 1982, NASA CR 165846.

11. Tingas, S. A. and Rao, D. M.; "Subsonic Balance and Pressure Investigation of a 60-Deg. Delta Wing with Leading-Edge Devices." 1982, NASA CR 165923.

12. Rao, D. M. and Johnson, T. D., Jr.; "Investigation of Delta Wing Leading-Edge Devices." J. Aircraft, Vol. 18, No. 3, March 1981.

13. Rao, D. M. and Johnson, T. D., Jr.; "Subsonic Pitch-Up Alleviation on a 74-Deg. Delta Wing." 1981, NASA CR 165749.

14. Rao, D. M.; "Leading-Edge Vortex Flap Experiments on a 74-Deg. Delta Wing." 1979, NASA CR 159161.

15. Rao, D. M.; "Exploratory Subsonic Investigation of Vortex Flap Concept on Arrow Wing Configuration." 1979, NASA CP 2108.

16. Rao, D. M.; "Leading-Edge Vortex Flaps for Enhanced Subsonic Aerodynamics of Slender Wings." 1980, ICAS 12th Congress, Paper 80-i3.5.

17. Smith, C. W., Campbell, J. F. and Huffmann, J. K.; "Experimental Results of a Leading-Edge Vortex Flap on a Highly Swept Cranked Wing." 1980, NASA CP 2162.

18. Lamar, J. E. and Campbell, J. F; "Design Related Study of Transonic Manauvering Slender Wings Having Vortex Flow." 1980, NASA CP 2162.

19. Yip, L. P. and Murri, D. G.; "Effect of Vortex Flaps on the Low-Speed Aerodynamic Characteristics of an Arrow Wing." 1981, NASA TP 1914.

20. Schoonover, W. E., Jr. and Ohlson, W. E.; "Wind Tunnel Investigation of Vortex Flaps on a Highly-Swept Interceptor Configuration." 1982, ICAS 13th Congress, Paper 82-6.7.3.

21. Frink, N. T.; "Analytical Study of Vortex Flaps on a Highly Swept Delta Wing." 1982, ICAS 13th Congress, Paper 82-6.7.2.

22. Marchman, J. F.; "Effectiveness of Leading-Edge Vortex Flaps on 60- and 75-Deg. Delta Wings." J. Aircraft, Vol. 18, No. 4, April 1981.

23. Marchman, J. F.; "The Aerodynamics of Inverted Leading Edge Vortex Flaps on Delta Wings." 1981, AIAA Paper 81-0356.

24. Frink, N. T., et al; "Vortex Flow Re-attachment Line and Subsonic Aerodynamic Data for Vortex Flaps on 50-Deg. to 74-Deg. Delta Wings on Common Fusalage." 1983, NASA TM 84618.

25. Rao, D. M.; "Upper Vortex Flap - A Versatile Surface for Highly Swept Wings.: 1982, ICAS 13th Congress, Paper 82-6.7.1.

26. Rao, D. M.; "Segmented Vortex Flaps." 1983, AIAA 21st Aerospace Sciences Meeting, Paper 83-0424.

27. Buter, T. A. and Rao, D. M.; "Experimental and Computational Investigation of an Apex Flap Concept on a 74° Delta Wing." NASA CR 166080, 1983.

28. Wentz, W. H., Jr.; "Effects of Leading-Edge Camber on Low Speed Characteristics of Slender Delta Wings." 1972, NASA CR 2002.

ACKNOWLEDGEMENT

The sustained encouragement and cooperation received by the author from collaagues at NTF Aerodynamics Branch, as well as the material support of Transonic Aerodynamics Division, NASA Langley Research Center, are gratefully acknowledged.

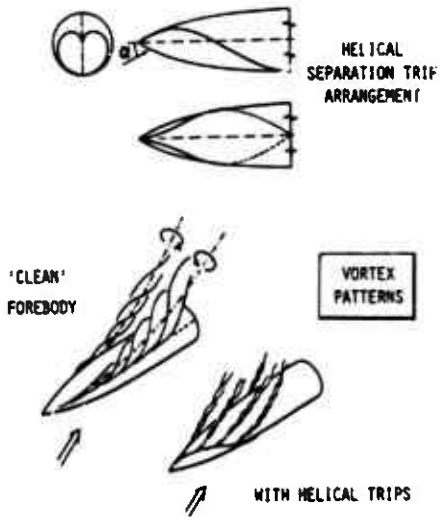

Fig. 1. Helical trip concept

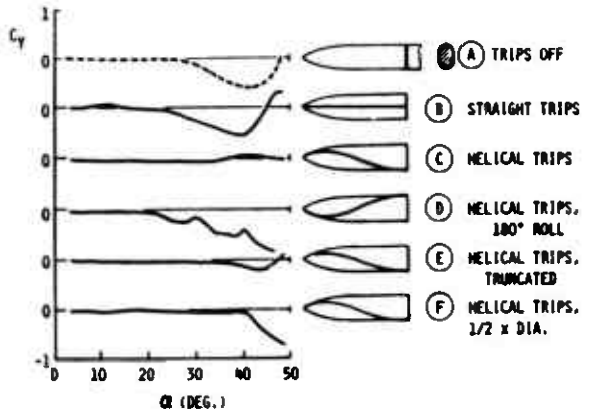

Fig. 2. Basic fuselage side force characteristics with helical and modified trips

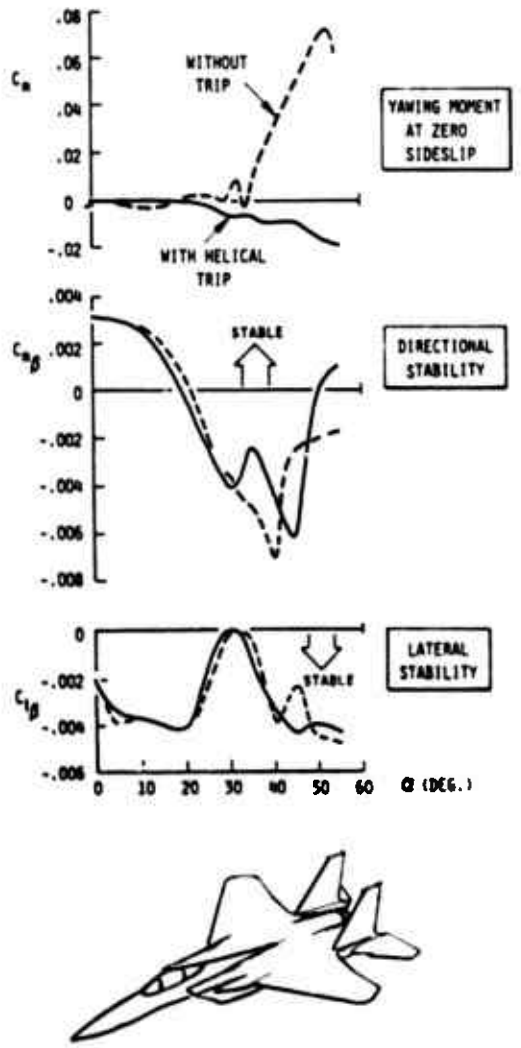

Fig. 3. Helical trip effectiveness on a fighter configuration (ref. 4)

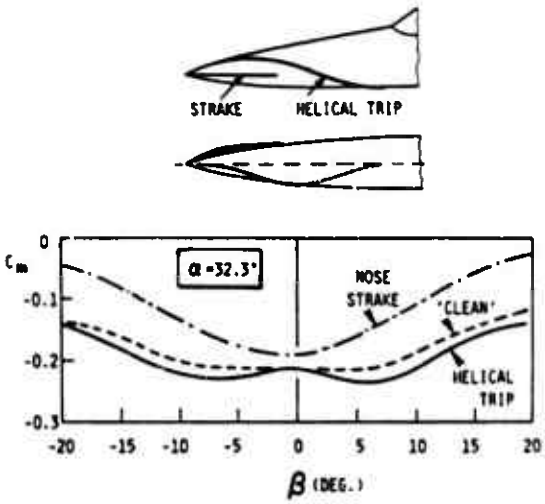

Fig. 4. Helical-trip and nose-strake effects on sideslip-induced pitching moment (fighter configuration, ref. 4)

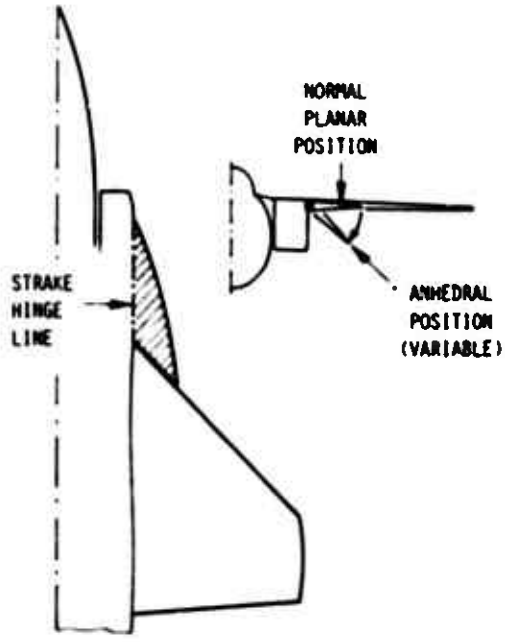

Fig. 5. Hinged strakes, shown in a hypothetical installation

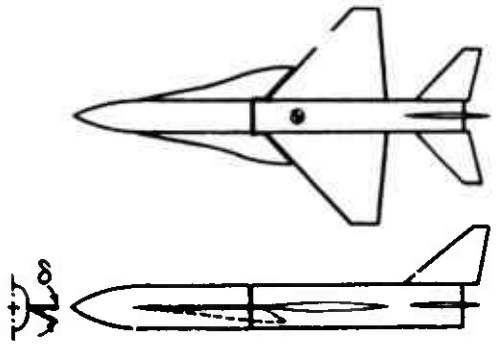

Fig. 6. Generic fighter model for hinged strake investigation

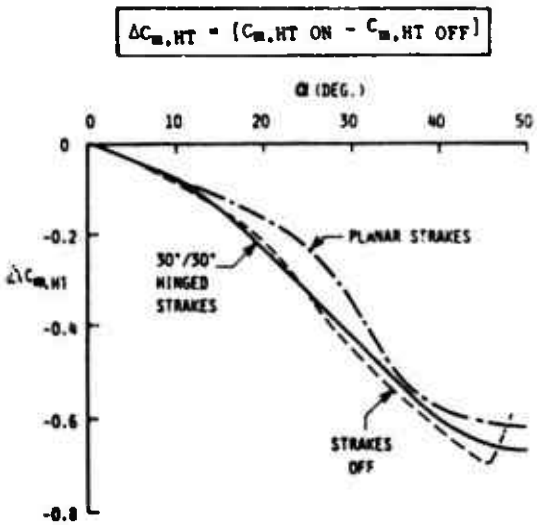

Fig. 8. Horizontal tail (HT) effectiveness with planar and anhedral strakes

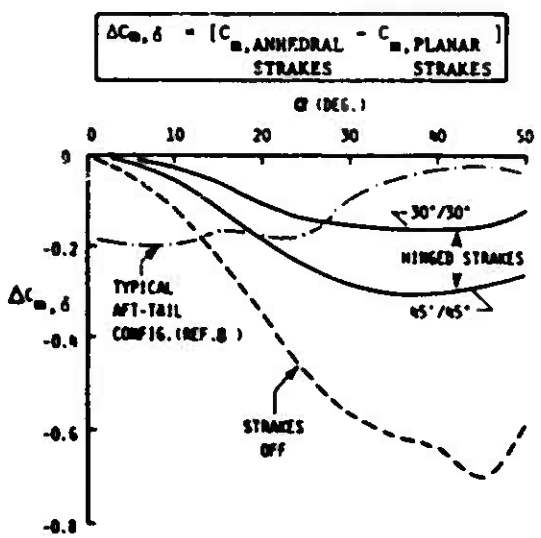

Fig. 9. Nose-down moment by anhedralling hinged strakes from planar position

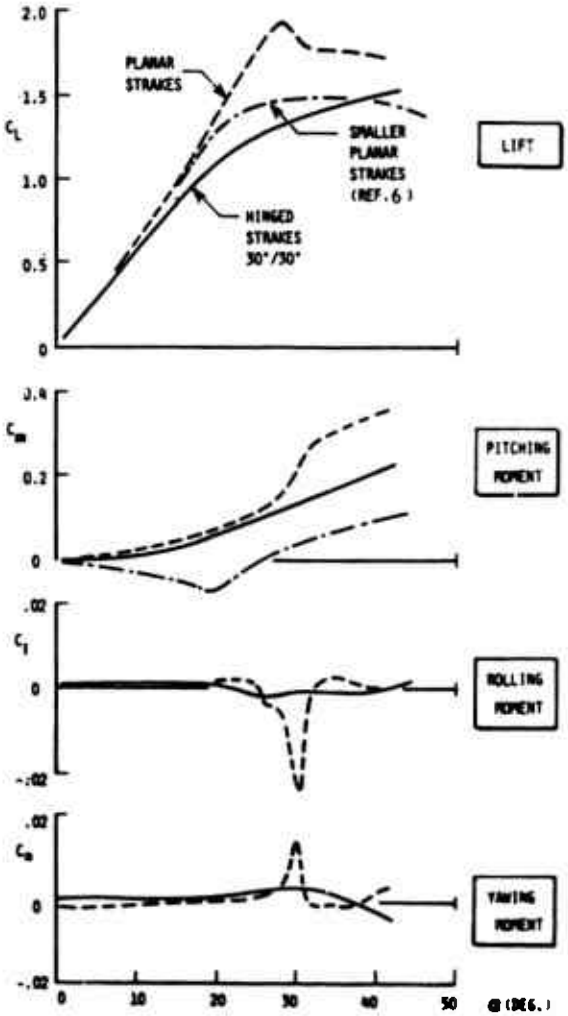

Fig. 7. Aerodynamic characteristics with planar and anhedral strakes

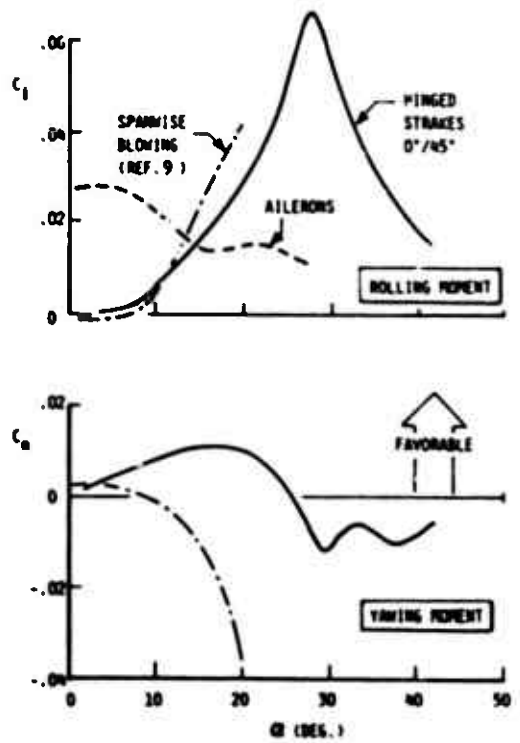

Fig. 10. Rolling moment and induced yaw due to asymmetric anhedral

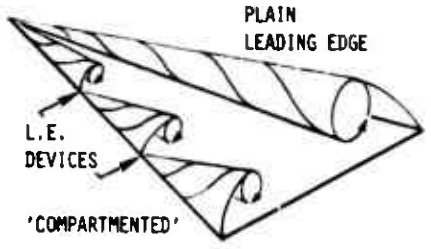

Fig. 11. 'Compartmentation' of swept leading edge separation

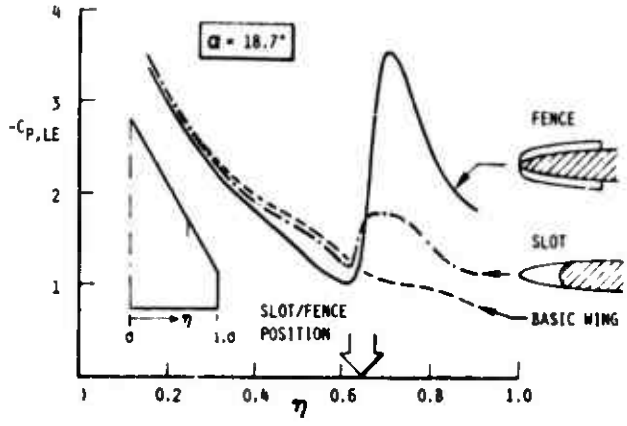

Fig. 12. Spanwise leading-edge pressure distribution with a slot or a fence

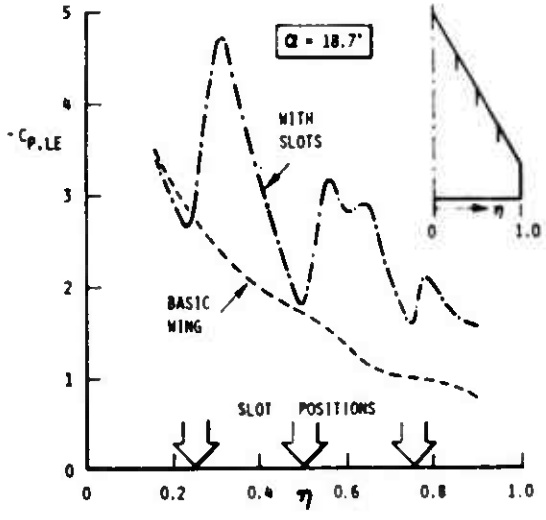

Fig. 13. Spanwise leading-edge pressure distribution with three slots

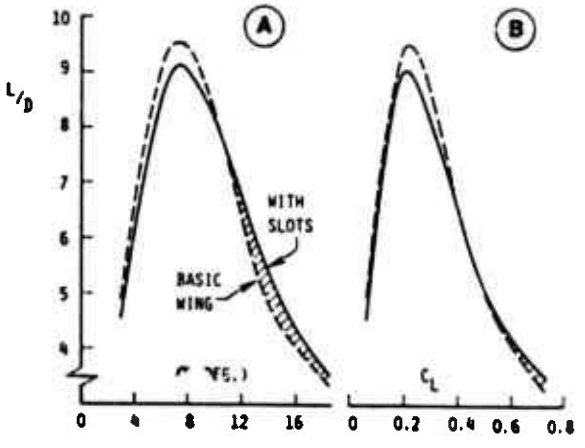

Fig. 14. Lift/drag ratio improvement with three slots

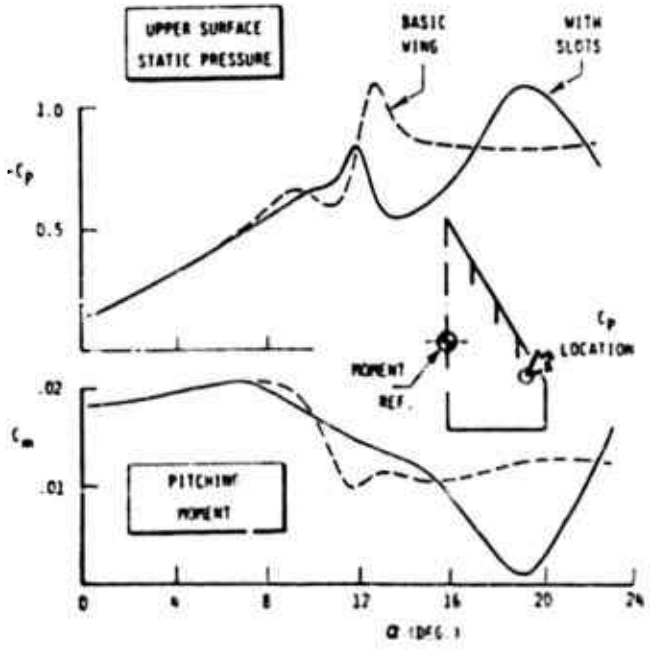

Fig. 15. Effect of three slots on upper-surface static pressure in tip region, and resulting pitching moment characteristics

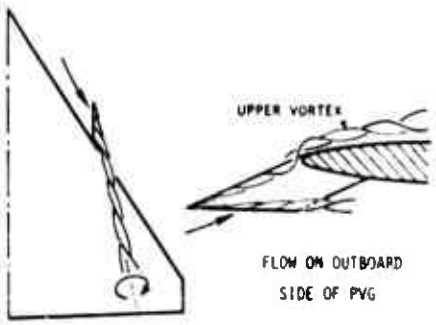

Fig. 16. Pylon vortex generator concept

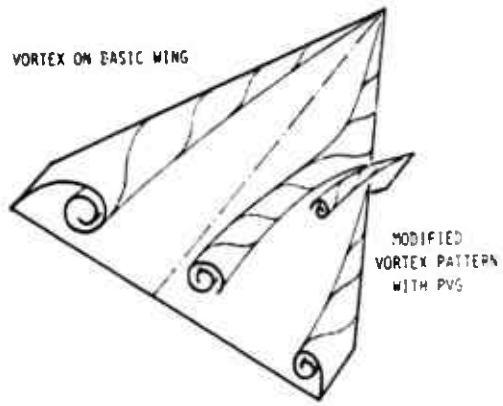

Fig. 17. Suggested leading-edge compartmentation mechanism of pylon vortex generator

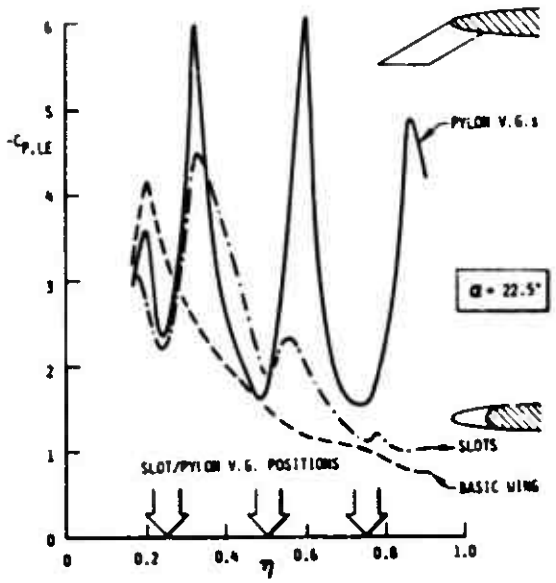

Fig. 18. Spanwise leading-edge pressure distribution at highest angle of attack with three PVGs

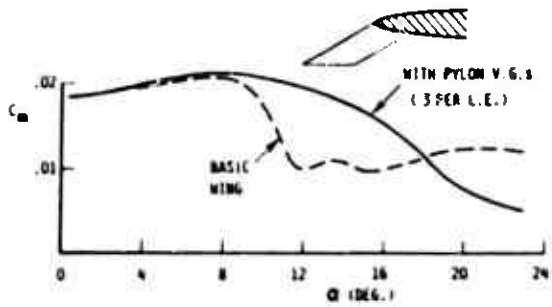

Fig. 19. Pitching-moment characteristics of 60-deg. delta with three PVGs

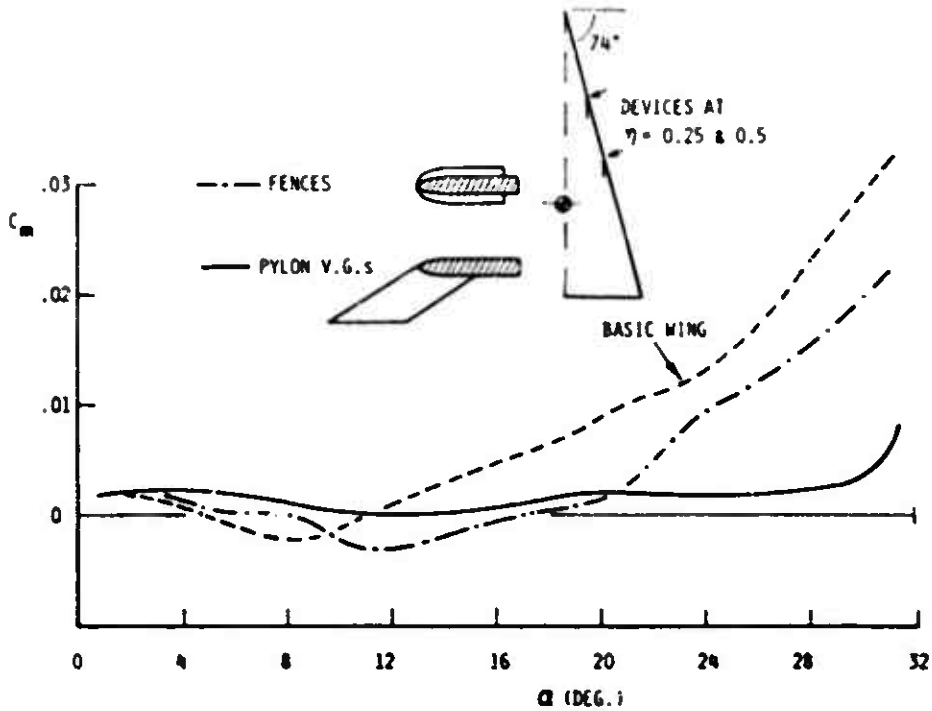

Fig. 20. Pitching-moment characteristics of 74-deg. delta with two PVGs

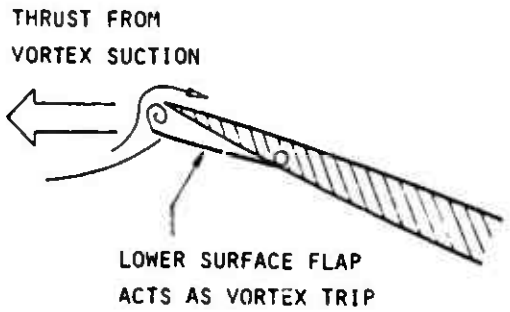

Fig. 21. Under-wing vortex trip concept

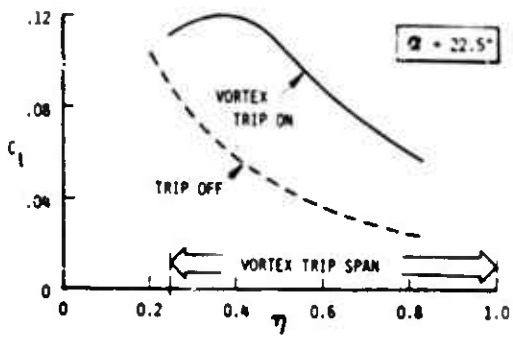

Fig. 23. Local leading-edge thrust distribution at highest angle of attack, showing effect of vortex trip

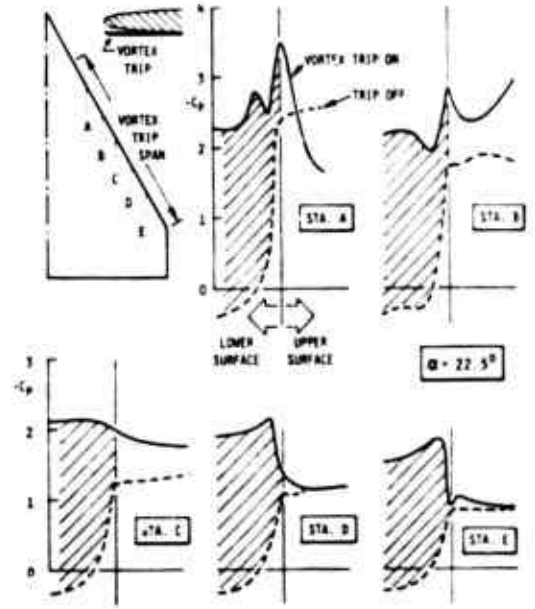

Fig. 22. Pressure distributions around leading edge at various semi-span stations, showing effect of vortex trip

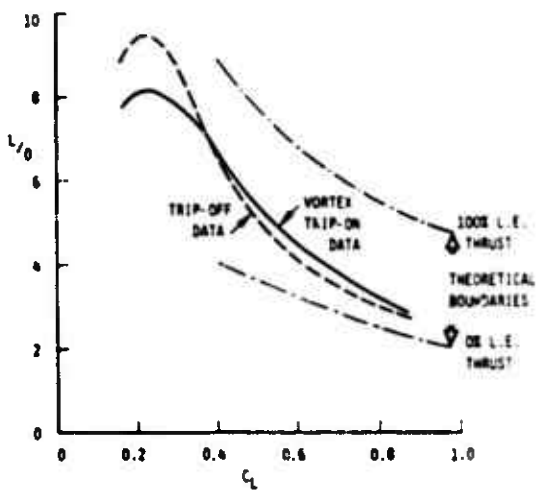

Fig. 24. Lift/drag ratio improvement due to vortex trip on 60-deg. delta

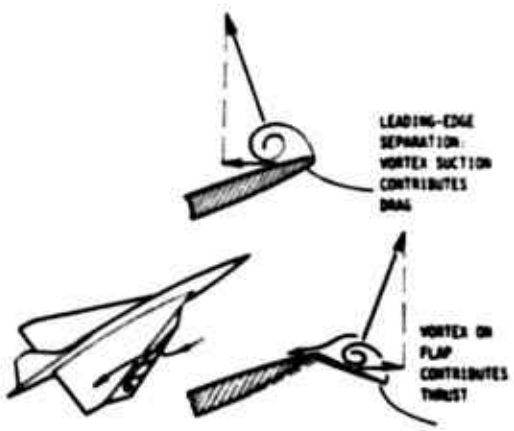

Fig. 25. Vortex flap concept

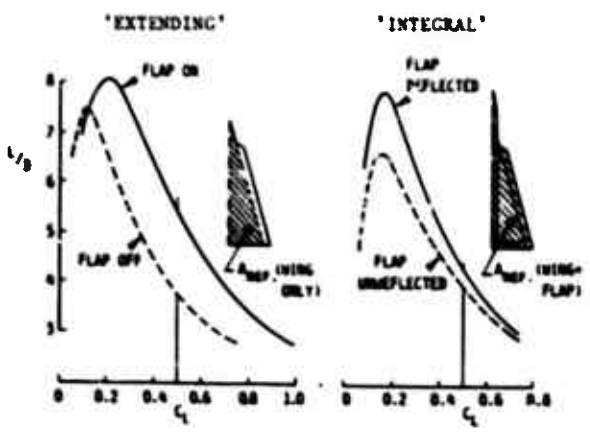

Fig. 26. Lift/drag ratio improvement due to 'extending' and 'integral' vortex flaps

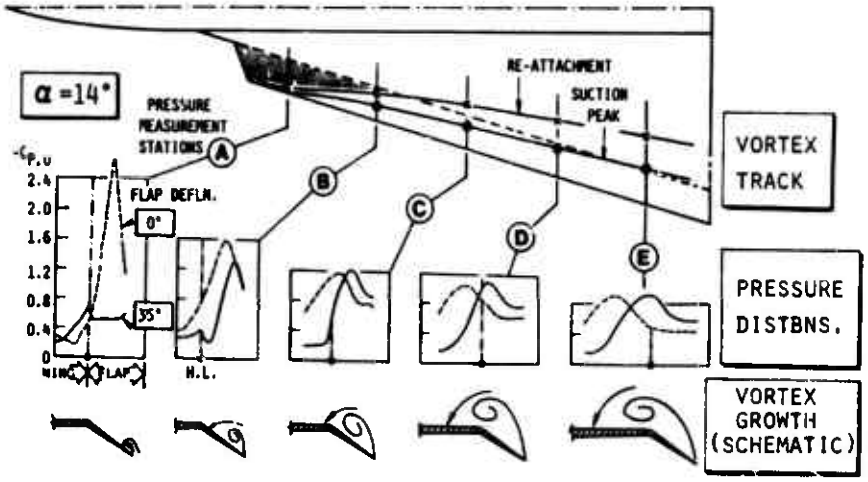

Fig. 27. Upper-surface pressure distributions at various spanwise stations showing vortex development

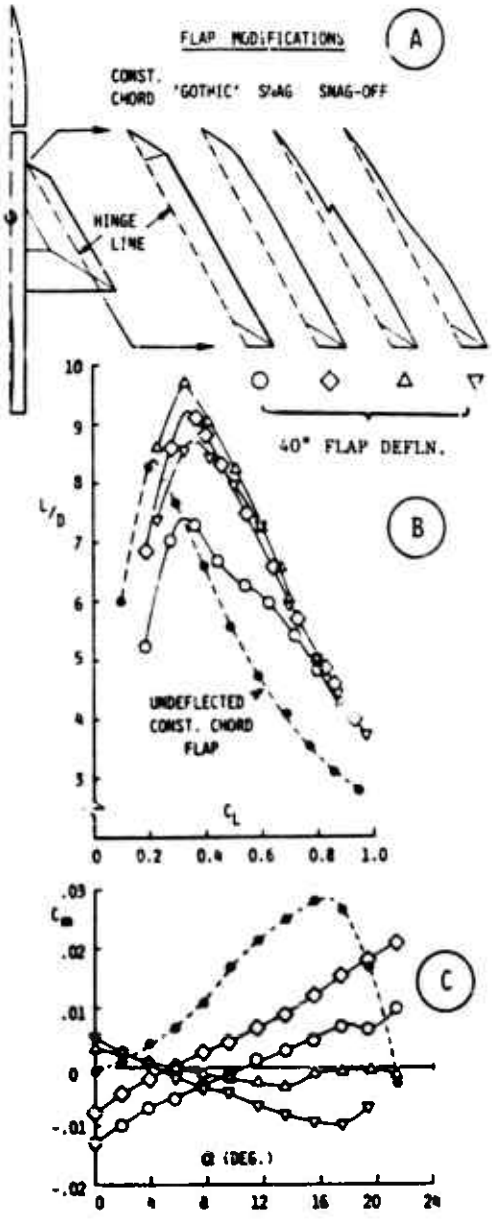

Fig. 28. Vortex flap modification effects on lift/drag ratio and pitching-moment characteristics

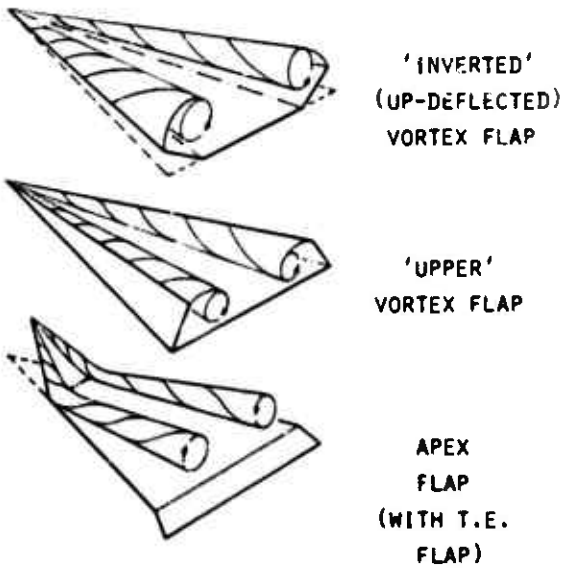

Fig. 29. Forced-vortex concepts for lift increase at low angles of attack

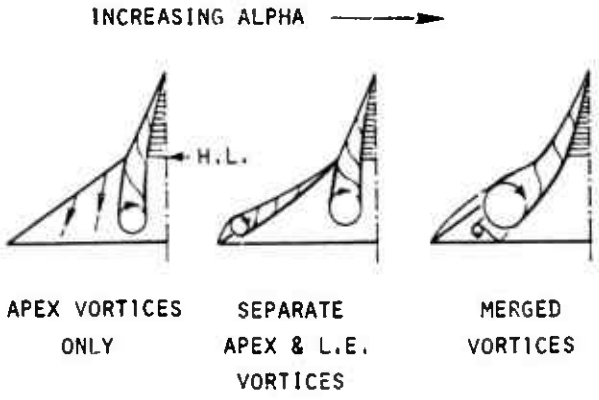

Fig. 30. Observed vortex patterns with deflected apex flap

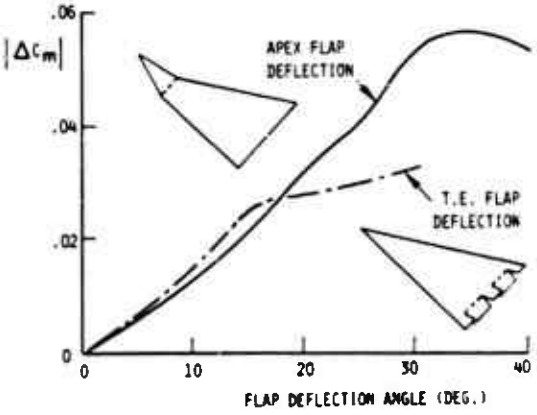

Fig. 31. Pitching-moment increments due to apex flap and trailing-edge flap

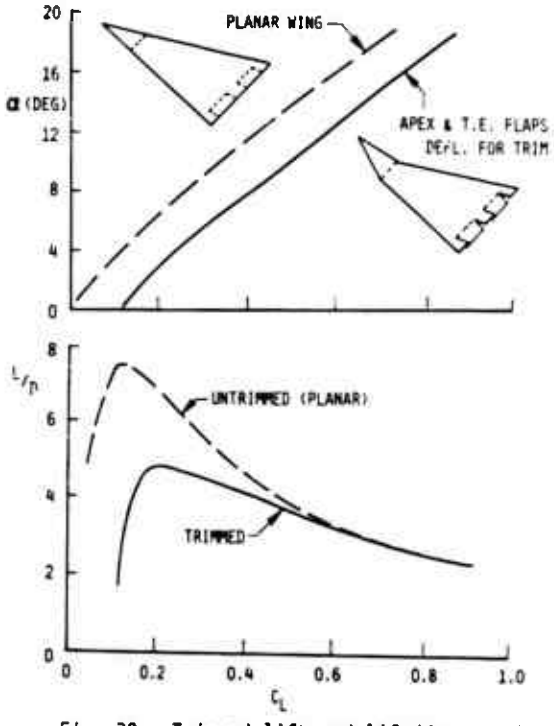

Fig. 32. Trimmed-lift and lift/drag ratio characteristics with apex flap and trailing-edge flap

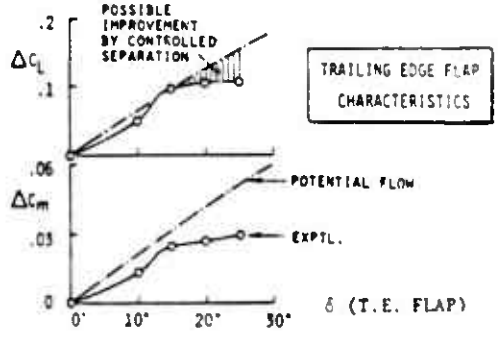

Fig. 33. Possible additional lift by maintaining attached flow on trailing-edge flap

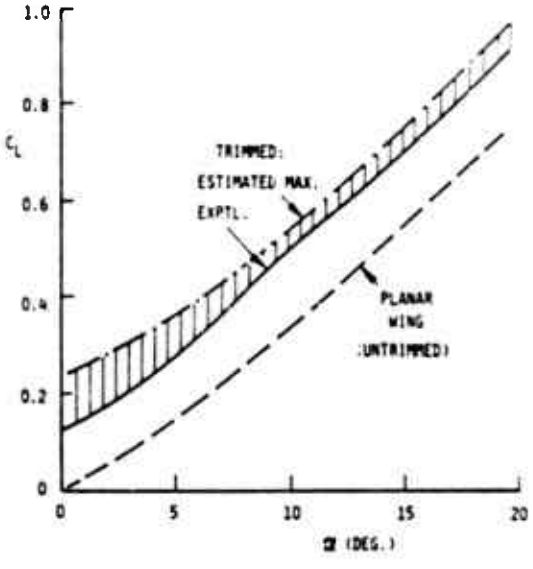

Fig. 34. Possible trimmed-lift increase with apex flap and unseparated trailing-edge flap

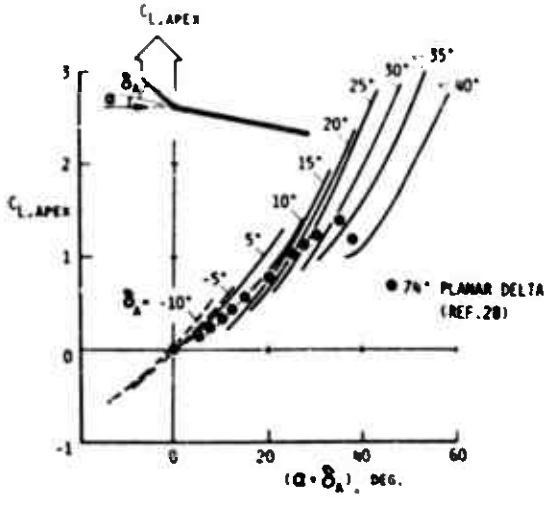

Fig. 35. Apex flap lift characteristics